nature medicine

ARTICLES

https://doi.org/10.1038/s41591-021-01515-2

Powered hip exoskeleton improves walking economy in individuals with above-knee amputation

Marshall K. Ishmael, Dante Archangeli and Tommaso Lenzi ✉

Above-knee amputation severely reduces the mobility and quality of life of millions of individuals. Walking with available leg prostheses is highly inefficient, and poor walking economy is a major problem limiting mobility. Here we show that an autonomous powered hip exoskeleton assisting the residual limb significantly improves metabolic walking economy by 15.6 ± 2.9% (mean ± s.e.m.; two-tailed paired *t*-test, $P = 0.002$) in six individuals with above-knee amputation walking on a treadmill. The observed metabolic cost improvement is equivalent to removing a 12-kg backpack from a nonamputee individual. All participants were able to walk overground with the exoskeleton, including starting and stopping, without notable changes in gait balance or stability. This study shows that assistance of the user's residual limb with a powered hip exoskeleton is a viable solution for improving amputee walking economy. By significantly reducing the metabolic cost of walking, the proposed hip exoskeleton may have a considerable positive impact on mobility, improving the quality of life of individuals with above-knee amputations.

Every year, 1 million lower-limb amputations occur worldwide[1]. After above-knee amputation, the biological ankle and knee are replaced by prosthetic joints that do not fully replicate the biomechanical functions of their biological counterparts[2]. Unlike biological legs, available knee and ankle prostheses cannot inject net-positive energy into the gait cycle. Individuals with above-knee amputations compensate for the lack of energy from the prosthesis by overexerting their residual-limb and intact-limb muscles[3–5]. These compensatory movements disrupt the natural efficiency of walking[3–5], increasing metabolic cost and severely reducing mobility and quality of life[6,7].

Biomechanical simulations and experiments with nonamputee individuals have shown that the ankle joint provides considerable net-positive energy during walking[8,9]. If the ankle is impaired or missing, as is the case after amputation, the individual must increase their residual-limb and intact-limb effort to compensate for the missing ankle energy, resulting in an unnatural, asymmetric and inefficient gait pattern[3]. As a result, walking with a prosthesis is slower, less stable and less efficient than nonamputee walking[5]. A recent wave of technological advances has enabled the development of powered knee and ankle joints that can theoretically replicate the biomechanical functions of the missing biological leg[10]. These emerging powered prostheses aim to restore natural walking efficiency by providing positive energy at the prosthetic joints. However, the required batteries and servomotors increase the mass of the prosthesis.

Adding mass to body segments increases the metabolic cost of walking. The increase in metabolic cost is proportional to the distance between the added mass and the user's body center of mass[11]. Consequently, adding mass at the ankle costs four times as much metabolic energy as adding mass at the trunk[11]. In addition, the entire mass of a prosthesis must be fully suspended through the residual limb, which causes problems with socket stability[12]. Therefore, the potential benefits of providing positive energy with powered prostheses are offset by the distal mass of these devices, which increases metabolic effort. Despite some recent success in reducing the weight of powered prostheses[13,14], no powered device has so far been able to consistently improve metabolic cost in individuals with above-knee amputation.

In this study, we investigate an alternative strategy to improve walking economy in individuals with above-knee amputations. Rather than restoring the energy injection from the missing biological leg with a powered prosthesis, we propose assisting the residual limb with an autonomous, powered hip exoskeleton (Fig. 1). Powered hip exoskeletons can be very lightweight because they only need to provide a fraction of the hip's biological torque to assist the residual limb. Furthermore, the mass of a hip exoskeleton creates less burden to the body because it is both lighter and located closer to the body's center of mass, minimizing the metabolic energy cost of carrying it[11]. Finally, because the hip exoskeleton is not suspended through a socket interface, socket stability issues may be reduced. Thus, the negative effects of wearing a powered hip exoskeleton are minimal. But can hip assistance compensate for the lack of energy at the ankle?

Powered prostheses aim to reduce the metabolic cost of walking by adding energy at the ankle joint, which is physiological. In contrast, the proposed exoskeleton approach aims to reduce the metabolic cost of walking by adding energy at the hip joint, which is non-physiological. Autonomous powered hip exoskeletons have successfully reduced the metabolic cost of walking[15] and even running[16] in young nonamputee individuals. However, whether hip exoskeletons can reduce metabolic cost in individuals with an above-knee amputation is unknown. Supported by pilot experiments[17,18], this study tests the hypothesis that a powered hip exoskeleton can reduce the metabolic cost of walking in individuals with above-knee amputations by injecting energy at the residual hip joint.

Results

We conducted experiments with individuals with above-knee amputation ($n = 6$) walking with and without an autonomous, unilateral powered hip exoskeleton (Fig. 1)[18]. All data from the following experiments are openly available[19]. The total weight of the autonomous exoskeleton was 2,451 g. All participants used their prescribed prostheses (Supplementary Table 1). Participants walked on a treadmill at a speed of 1 m s^{-1} and overground on a 12-m walkway (Supplementary Videos 1 and 2). The powered hip exoskeleton provided assistive torque in flexion and extension. The peaks of

Department of Mechanical Engineering and Robotics Center, University of Utah, Salt Lake City, UT, USA. ✉e-mail: t.lenzi@utah.edu

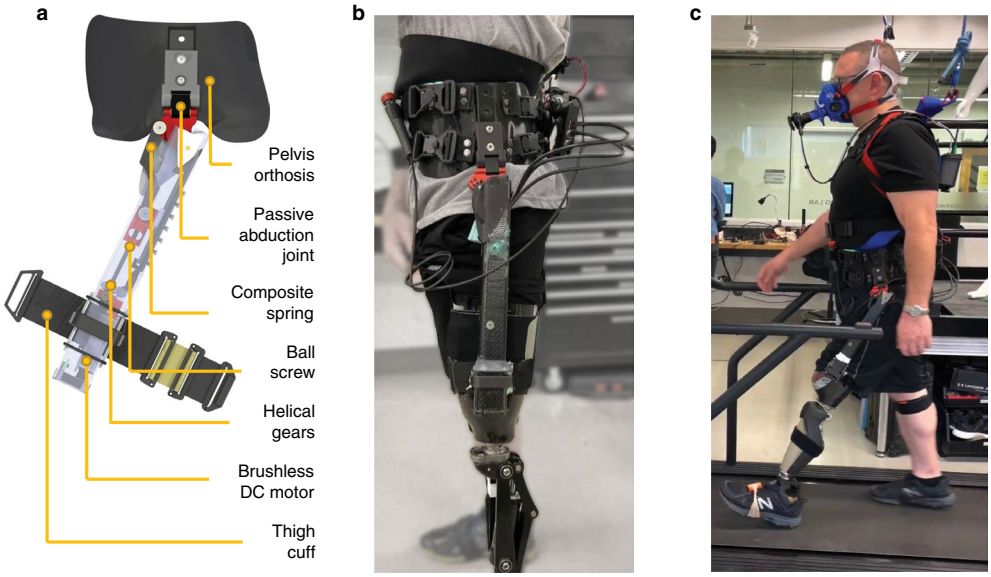

Fig. 1 | Powered hip exoskeleton and experimental setup. a, A model of the powered hip exoskeleton with transparency to show the actuation system. The exoskeleton comprises a three-dimensionally (3D)-printed orthosis strapped to the pelvis and a flexible cuff attached to the residual limb by wrapping around the socket. The actuation system comprises a brushless DC motor, helical gears, a ball screw and a composite spring. A passive abduction/adduction joint acts in series to the powered flexion/extension joint. **b**, Close-up view of the exoskeleton on a participant. **c**, Participant walking with the exoskeleton on a treadmill while wearing a portable calorimetry system and a safety harness.

flexion and extension and their respective timing were manually tuned for each participant based on their subjective preferences as well as the experience of the experimenter. Metabolic energy consumption was measured using indirect calorimetry during the treadmill test. To avoid any potential confounding effects, participants were not allowed to use the treadmill's handrails.

Treadmill test. The metabolic cost of walking was calculated for each participant as the total metabolic energy consumption minus the metabolic consumption measured during relaxed standing[11]. The total metabolic energy consumption was $4.41 \pm 0.40\,W\,kg^{-1}$ (mean ± standard error of the mean (s.e.m.)) with the exoskeleton and $4.95 \pm 0.39\,W\,kg^{-1}$ without the exoskeleton (Fig. 2). The metabolic consumption measured during relaxed standing was $1.43 \pm 0.08\,W\,kg^{-1}$. Thus, the powered hip exoskeleton reduced the metabolic cost of walking by 15.6 ± 2.9% on average across the six participants (paired *t*-test, $P = 0.002$). All six participants showed a reduction in the metabolic cost of walking with the powered hip exoskeleton compared to walking without the exoskeleton (Fig. 2 and Supplementary Table 2).

We computed the average hip, knee and ankle angles across all participants by considering the last 20 strides of the treadmill walking session with the exoskeleton (Fig. 3, red line) and without the exoskeleton (Fig. 3, gray line). The range of motion of the residual hip joint was significantly larger (6.42%, $P = 0.004$) with the exoskeleton than without the exoskeleton (Fig. 3 and Supplementary Table 3). Specifically, the range of motion of the residual hip was 49.42° and 46.54° with and without the exoskeleton, respectively. No significant differences were observed in the range of motion of the intact limb or the prosthesis joints ($P > 0.01$; Fig. 3 and Supplementary Table 3). Also, we analyzed temporal gait symmetry and movement of the center of mass and did not find significant differences with and without the exoskeleton ($P > 0.01$, Supplementary Tables 3 and 4). Thus, only the residual hip kinematics were significantly affected by the exoskeleton assistance.,

The residual hip joint kinematics with exoskeleton assistance varied noticeably between participants. The hip range of motion ranged between 37.97° and 59.08° (Fig. 4a). The peak of the flexion torque ranged between 0.088 and $0.122\,Nm\,kg^{-1}$, whereas the peak of the extension torque ranged between −0.049 and $-0.092\,Nm\,kg^{-1}$. Flexion torque peaked between 56.7 and 64.2% of stride, and extension torque peaked between 9.4 and 14.3% of stride (Fig. 4b). The resulting peaks for exoskeleton hip joint power were $0.404 \pm 0.034\,W\,kg^{-1}$ and $0.14 \pm 0.018\,W\,kg^{-1}$ in flexion and extension, respectively (Fig. 4c). As a result, on average, 69.0% of the exoskeleton assistive energy occurred during flexion (Fig. 4d,e). On average, across all participants, the powered hip exoskeleton injected $0.100 \pm 0.007\,J\,kg^{-1}$ per stride at the residual hip, ranging between 0.082 and $0.134\,J\,kg^{-1}$ per stride (Fig. 4f).

Overground test. All participants walked overground with and without the exoskeleton at their self-selected speed. The tuning of exoskeleton assistance was kept the same as for the treadmill test. However, on average, participants walked faster than $1\,m\,s^{-1}$ (Supplementary Table 4)—the fixed speed used during the treadmill test. Because of the faster self-selected walking speed, the assistive power of the exoskeleton was higher overground than on the treadmill. Specifically, the peak power was $0.157 \pm 0.007\,W\,kg^{-1}$ and $0.427 \pm 0.033\,W\,kg^{-1}$ in extension and flexion, respectively. However, the energy injected by the exoskeleton overground ($0.105 \pm 0.006\,J\,kg^{-1}$ per stride) was approximately the same as during the treadmill test ($0.100 \pm 0.007\,J\,kg^{-1}$ per stride). The range of motion of the residual hip joint was larger with the exoskeleton than without the exoskeleton (10.6%, 3.91°), although, unlike in the treadmill test, this difference was not statistically significant ($P = 0.055$). No significant differences were observed in walking speed, center-of-mass kinematics or temporal gait symmetry with and without the exoskeleton.

Discussion

To date, the most metabolically efficient device for individuals with above-knee amputation is a microprocessor-controlled prosthesis, a technology introduced to the market in the 1990s. Compared to the previous generation of prostheses, which were introduced in

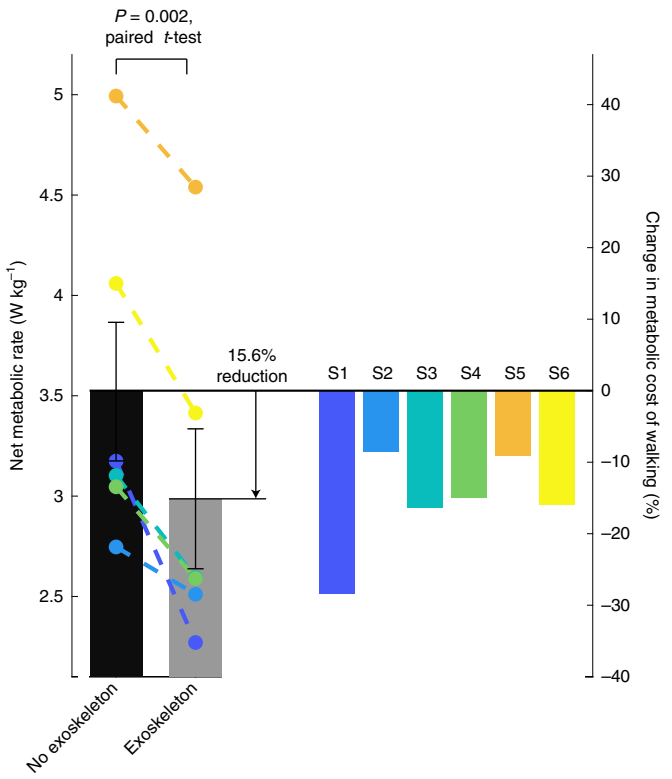

Fig. 2 | Metabolic cost of walking with and without the exoskeleton. Black and gray bars represent the net metabolic rate in W kg^{-1} averaged across all participants ($n=6$) with and without the exoskeleton, respectively. Error bars show the s.e.m. for each condition. The square bracket shows the result of a paired two-sided t-test ($t=5.837$, degrees of freedom (df) = 5, $P=0.002$ (0.299, 0.769)). Colored dots represent the net metabolic rate for each participant with and without the exoskeleton in W kg^{-1}. Colored bars represent the percent change in the net metabolic rate of walking with the exoskeleton, where negative values indicate a reduction in the metabolic cost of walking. The vertical arrow indicates the reduction in metabolic cost averaged across all participants (15.6%, $n=6$).

the 1950s[20], microprocessor-controlled prostheses improve walking economy by 5–6.5% (refs. [21,22]). The proposed autonomous powered hip exoskeleton improves walking economy by 15.6%, compared to walking with a prosthesis alone. The observed metabolic cost reduction is equivalent to removing a 12-kg backpack from a nonamputee individual[11], and is greater than any metabolic cost reductions observed with an autonomous exoskeleton in nonamputee individuals[23], with the exception of one study[15]. All participants were able to walk overground with the exoskeleton, including starting and stopping, without noticeable changes in gait balance or stability. By significantly reducing the metabolic cost of walking, the proposed hip exoskeleton may have a considerable positive impact on mobility, improving the quality of life of individuals with above-knee amputations[6,7].

In nonamputee individuals walking at 1.36 m s^{-1}, the biological hip and the biological ankle provide 0.157 J kg^{-1} and 0.288 J kg^{-1} positive energy per stride, respectively[3]. In individuals with above-knee amputation walking at 1.2 m s^{-1} with passive prostheses and without exoskeleton assistance, the residual hip and the prosthetic ankle provide 0.192 J kg^{-1} and 0.063 J kg^{-1} of positive energy per stride, respectively[3]. Thus, the residual hip in individuals with amputations produces more positive energy than the intact hip in nonamputee individuals (0.192 J kg^{-1} versus 0.157 J kg^{-1}). However, the combined residual hip and prosthetic ankle in individuals with amputations produces lower positive energy than the combined intact hip and ankle joint energy in nonamputee individuals (that is, 0.255 J kg^{-1} versus 0.445 J kg^{-1}). This study shows that, by injecting energy at the residual hip, the proposed autonomous powered hip exoskeleton can compensate for the observed deficiency in total joint energy, improving walking economy in individuals with above-knee amputations.

Biomechanics studies have shown that individuals with above-knee amputation overexert both the residual and contralateral hip, with 0.192 J kg^{-1} and 0.231 J kg^{-1}, respectively, versus 0.157 J kg^{-1} for nonamputee individuals[3]. Thus, bilateral assistance may lead to higher metabolic saving compared to that observed in this study by additionally compensating for the compensatory action of the contralateral hip joint (that is, the sound-side hip joint). On the other hand, a bilateral exoskeleton will be heavier and more intrusive for the user than the proposed unilateral hip exoskeleton. Thus, it is not clear that bilateral assistance could be more effective than unilateral assistance.

In this study, the hip assistance was manually tuned for each participant by the experimenter, who relied on their experience and subjective feedback from the participants. The manual tuning took about 15 min, during which participants walked for less than 10 min in 2- to 3-min bouts. Although the manual tuning aimed to maximize the exoskeleton assistance in both flexion and extension, participants consistently preferred higher flexion than extension assistance (0.10 ± 0.005 Nm kg^{-1} versus 0.07 ± 0.006 Nm kg^{-1}). Studies using powered exoskeletons with nonamputee individuals have presented control algorithms that automatically optimize the exoskeleton assistance as the person walks to minimize metabolic cost[24,25]. This automatic tuning approach may lead to optimal assistance and, therefore, a greater metabolic cost reduction than what we observed in this study. However, automatic optimal tuning requires more walking (that is, 64 min[24] and 21 min[25]) than the manual, non-optimal tuning used in this study (that is, <10 min), and a longer tuning time may present a challenge for the population with amputations. Moreover, automatic tuning does not explicitly consider subjective preference. These shortcomings may explain why automatic tuning was not successful at reducing the metabolic cost of walking in individuals with amputations[26].

To allow for sufficient time for learning, participants walked for 18 min with the powered exoskeleton assistance, divided into three 6-min walking sessions, and data were collected during the last 2 min of the third walking session. Thus, the time necessary to adapt to the assistance provided by a powered exoskeleton is relatively short and should not limit the clinical viability of the proposed assistive approach. Interestingly, sensory feedback restoration has been shown to improve metabolic cost during walking with a microprocessor-controlled prosthesis[27]. Thus, combining a powered hip exoskeleton and sensory feedback restoration may lead to even greater metabolic cost reduction than that observed in this study.

This study suggests that 10–15 Nm of peak torque is sufficient to obtain significant metabolic improvements. This level of torque is considerably lower than the maximum torque capacity of our autonomous powered hip exoskeleton (that is, 45 Nm[18]). Using 10–15 Nm as the maximum torque requirement may result in a lighter exoskeleton than the one used in this study, potentially leading to further metabolic cost improvements. Based on our pilot studies, providing greater torque than the level used in this study (Fig. 4b) resulted in uncomfortable movements of the socket. This problem may be addressed in the future by surgical interventions such as osseointegration[28] or thighplasty[29]. If we could increase the assistive torque while maintaining user comfort, we could increase the energy injected by the powered exoskeleton, further reducing the metabolic cost of walking[30].

This study shows that powered exoskeletons hold great potential for establishing a new standard of care for individuals with amputation. However, there are limitations that need to be considered. The

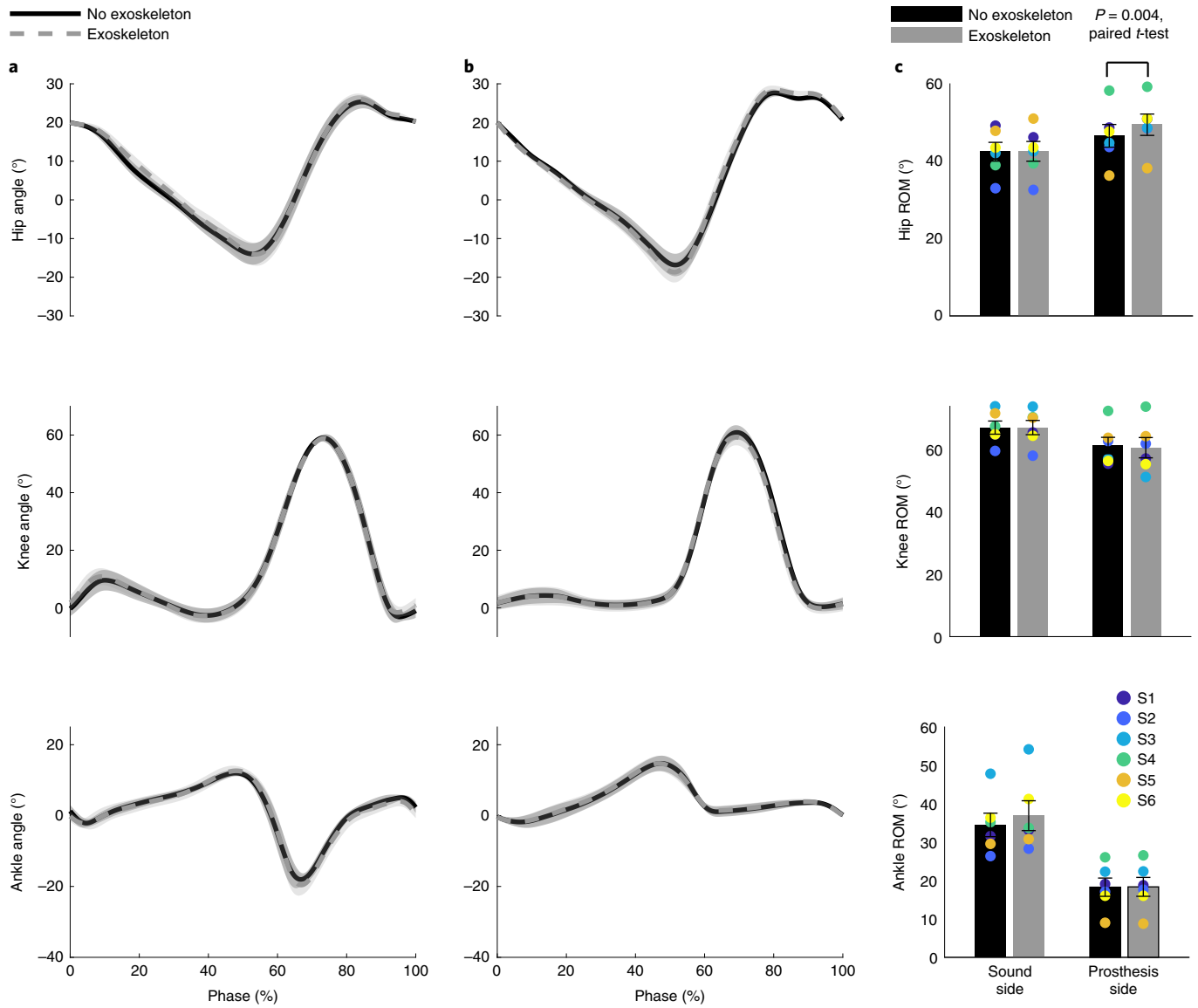

Fig. 3 | Lower-limb kinematics averaged across all participants. a,**b**, Kinematics of the sound side (**a**) and prosthesis side (**b**) are shown in the left and right columns, respectively (mean ± s.e.m.). The joint kinematic profiles with and without the exoskeleton are shown using dashed light gray and solid dark gray lines, respectively ($n = 6$, mean ± s.e.m.). **c**, Range of motion (ROM) for all joints, averaged across participants, is shown (mean ± s.e.m.), with the individual range of motion for each participant plotted in the corresponding color. The square bracket indicates a statistically significance difference ($n = 6$ participants; paired t-test: $t = 4{,}953$, df = 5, $P = 0.004$ (−4.372, −1.384)).

most important limitation of the study is that the sample population was relatively small ($n = 6$) and homogeneous (Medicare Functional Classification K Level 3 (K3) only[31,32], traumatic amputation only). Although it is clear from this study that energy injection at the residual limb reduces the metabolic cost of walking, we still lack a mechanistic explanation for the observed metabolic improvements, including an assessment of the relative contribution of flexion and extension assistance. Because the mechanics of treadmill and overground gait are very similar[33], we expect the walking economy improvements observed on the treadmill to extend to overground walking. However, we do not know whether these results will extend to inclined and uneven terrains, which are common in real life. Participants commented on the intuitiveness of walking with the exoskeleton and consistently reported that, after doffing the exoskeleton at the end of the experiment, walking without the exoskeleton felt considerably harder. Although this subjective feedback is encouraging, we still lack a quantitative assessment of subjective preference, which is essential for acceptability in real life.

Future clinical studies should assess the efficacy of the proposed intervention on a broader population of individuals with amputations, including different K levels (for example, K2/K3), different levels of amputation (for example, hip/knee disarticulation), different ambulation tasks (for example, walking on uneven terrain) and different levels of assistance. Also, future studies should assess joint-level torque and effort through inverse dynamics and electromyography, providing a mechanistic explanation for the observed metabolic improvements. A standard survey (for example, System Usability Scale) should be used to quantify subjective preference, assessing usability in real life. It would also be interesting to explore the trade-offs between bilateral and unilateral assistance, potentially combined with powered and passive prostheses. This knowledge will support engineering optimization of the proposed assistive

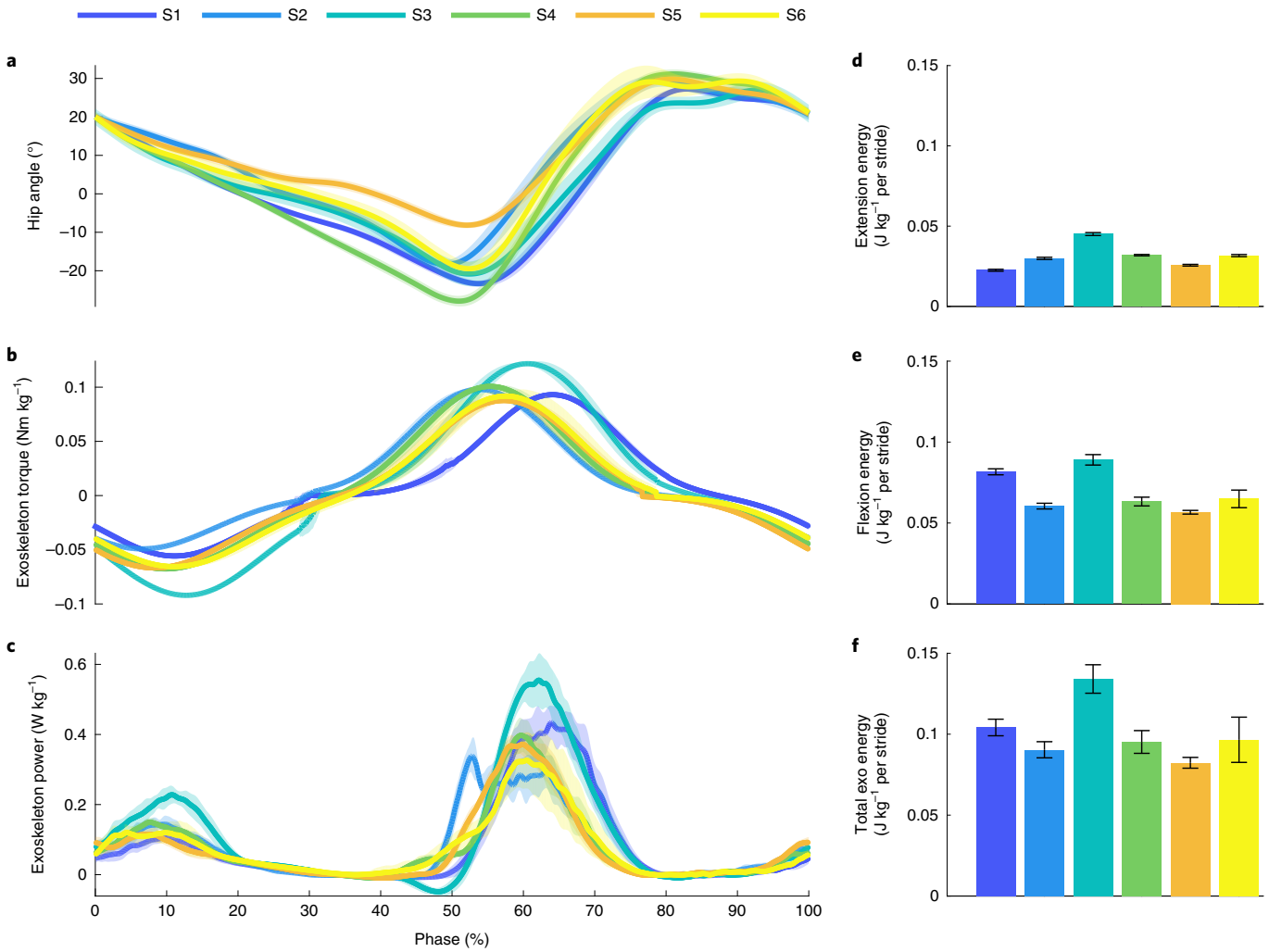

Fig. 4 | Average kinematics, kinetics and energy injection during walking with the exoskeleton on a treadmill at 1 m s^{-1}. Mean (solid lines) and s.d. (shaded areas) are shown over $n = 20$ strides for each participant. **a**, Measured residual hip angle normalized to stride duration. **b**, Exoskeleton torque normalized to body mass and stride duration. **c**, Power provided by the exoskeleton normalized to body mass and stride duration. **d**,**e**, Exoskeleton energy injected during hip extension (**d**) and flexion (**e**) normalized to body mass, respectively. **f**, Cumulative exoskeleton energy injected per stride normalized to body mass. All bar plots (**d**–**f**) display mean and s.d. for $n = 20$ strides for each participant.

device, which should focus on mechanically integrating the exoskeleton with the socket. We expect device optimization to be critical for the clinical success of the proposed intervention.

Online content

Any methods, additional references, Nature Research reporting summaries, source data, extended data, supplementary information, acknowledgements, peer review information; details of author contributions and competing interests; and statements of data and code availability are available at https://doi.org/10.1038/s41591-021-01515-2.

Received: 18 December 2020; Accepted: 19 August 2021;
Published online: 11 October 2021

References

1. Boulton, A. J., Vileikyte, L., Ragnarson-Tennvall, G. & Apelqvist, J. The global burden of diabetic foot disease. *Lancet* **366**, 1719–1724 (2005).
2. Goldfarb, M. Consideration of powered prosthetic components as they relate to microprocessor knee systems. *J. Prosthet. Orthot.* **25**, P65–P75 (2013).
3. Seroussi, R. E., Gitter, A., Czerniecki, J. M. & Weaver, K. Mechanical work adaptations of above-knee amputee ambulation. *Arch. Phys. Med. Rehabil.* **77**, 1209–1214 (1996).
4. Schmalz, T., Blumentritt, S. & Jarasch, R. Energy expenditure and biomechanical characteristics of lower limb amputee gait: the influence of prosthetic alignment and different prosthetic components. *Gait Posture* **16**, 255–263 (2002).
5. Waters, R. L. et al. Energy cost of walking of amputees: the influence of level of amputaton. *J. Bone Jt. Surg. Am.* **58**, 42–46 (1976).
6. Pell, J. P., Donnan, P. T., Fowkes, F. G. & Ruckley, C. V. Quality of life following lower limb amputation for peripheral arterial disease. *Eur. J. Vasc. Surg.* **7**, 448–451 (1993).
7. Wurdeman, S. R., Stevens, P. M. & Campbell, J. H. Mobility Analysis of AmpuTees (MAAT I): quality of life and satisfaction are strongly related to mobility for patients with a lower limb prosthesis. *Prosthet. Orthot. Int.* **42**, 498–503 (2018).
8. Sasaki, K., Neptune, R. R. & Kautz, S. A. The relationships between muscle, external, internal and joint mechanical work during normal walking. *J. Exp. Biol.* **212**, 738–744 (2009).
9. Farris, D. J. & Sawicki, G. S. The mechanics and energetics of human walking and running: a joint level perspective. *J. R. Soc. Interface* **9**, 110–118 (2012).
10. Goldfarb, M., Lawson, B. E. & Shultz, A. H. Realizing the promise of robotic leg prostheses. *Sci. Transl. Med.* **5**, 210ps15 (2013).

11. Browning, R. C., Modica, J. R., Kram, R. & Goswami, A. The effects of adding mass to the legs on the energetics and biomechanics of walking. *Med. Sci. Sports Exerc.* **39**, 515–525 (2007).
12. Alimusaj, M., Fradet, L., Braatz, F., Gerner, H. J. & Wolf, S. I. Kinematics and kinetics with an adaptive ankle foot system during stair ambulation of transtibial amputees. *Gait Posture* **30**, 356–363 (2009).
13. Tran, M., Gabert, L., Cempini, M. & Lenzi, T. A lightweight, efficient fully powered knee prosthesis with actively variable transmission. *IEEE Robot. Autom. Lett.* **4**, 1186–1193 (2019).
14. Gabert, L., Hood, S., Tran, M., Cempini, M. & Lenzi, T. A compact, lightweight robotic ankle–foot prosthesis: featuring a powered polycentric design. *IEEE Robot. Autom. Mag.* **27**, 87–102 (2020).
15. Seo, K., Lee, J., Lee, Y., Ha, T. & Shim, Y. Fully autonomous hip exoskeleton saves metabolic cost of walking. in *2016 IEEE International Conference on Robotics and Automation (ICRA)* 4628–4635 (IEEE, 2016).
16. Kim, J. et al. Reducing the metabolic rate of walking and running with a versatile, portable exosuit. *Science* **365**, 668–672 (2019).
17. Martini, E. et al. Lower-limb amputees can reduce the energy cost of walking when assisted by an Active Pelvis Orthosis. in *2020 8th IEEE RAS/EMBS International Conference for Biomedical Robotics and Biomechatronics (BioRob)* 809–815 (IEEE, 2020); https://doi.org/10.1109/BioRob49111.2020.9224417
18. Ishmael, M. K., Tran, M. & Lenzi, T. ExoProsthetics: assisting above-knee amputees with a lightweight powered hip exoskeleton. in *2019 IEEE 16th International Conference on Rehabilitation Robotics (ICORR)* 925–930 (IEEE, 2019).
19. Ishmael, M. K., Archangeli, D. & Lenzi, T. Powered hip exoskeleton improves walking economy in individuals with above-knee amputation. *figshare* https://doi.org/10.6084/m9.figshare.15180711 (2021).
20. Murphy, E. Hans Adolph Mauch. in *Memorial Tributes* **3**, 259–265 (National Academy of Engineering, 1989).
21. Johansson, J. L., Sherrill, D. M., Riley, P. O., Bonato, P. & Herr, H. P. A clinical comparison of variable-damping and mechanically passive prosthesis knee devices. *Am. J. Phys. Med. Rehabil.* **84**, 563–575 (2005).
22. Schmalz, T., Blumentritt, S. & Jarasch, R. Energy expenditure and biomechanical characteristics of lower limb amputee gait. *Gait Posture* **16**, 255–263 (2002).
23. Sawicki, G. S., Beck, O. N., Kang, I. & Young, A. J. The exoskeleton expansion: improving walking and running economy. *J. Neuroeng. Rehabil.* https://doi.org/10.1186/s12984-020-00663-9 (2020).
24. Zhang, J. et al. Human-in-the-loop optimization of exoskeleton assistance during walking. *Science* **356**, 1280–1283 (2017).
25. Ding, Y., Kim, M., Kuindersma, S. & Walsh, C. J. Human-in-the-loop optimization of hip assistance with a soft exosuit during walking. *Sci. Robot.* **3**, eaar5438 (2018).
26. Welker, C. G., Voloshina, A. S., Chiu, V. L. & Collins, S. H. Shortcomings of human-in-the-loop optimization of an ankle–foot prosthesis emulator: a case series. *R. Soc. Open Sci.* **8**, rsos.202020 (2021).
27. Petrini, F. M. et al. Sensory feedback restoration in leg amputees improves walking speed, metabolic cost and phantom pain. *Nat. Med.* **25**, 1356–1363 (2019).
28. Khemka, A., Frossard, L., Lord, S. J., Bosley, B. & Al Muderis, M. Osseointegrated total knee replacement connected to a lower limb prosthesis: 4 cases. *Acta Orthop.* **86**, 740–744 (2015).
29. Kuiken, T. A., Fey, N. P., Reissman, T., Finucane, S. B. & Dumanian, G. A. Innovative use of thighplasty to improve prosthesis fit and function in a transfemoral amputee. *Plast. Reconstr. Surg. Glob. Open* **6**, e1632 (2018).
30. Quinlivan, B. T. et al. Assistance magnitude versus metabolic cost reductions for a tethered multiarticular soft exosuit. *Sci. Robot.* **2**, eaah4416 (2017).
31. Hafner, B. J. & Smith, D. G. Differences in function and safety between Medicare Functional Classification Level-2 and -3 transfemoral amputees and influence of prosthetic knee joint control. *J. Rehabil. Res. Dev.* **46**, 417–434 (2009).
32. Gailey, R. S. et al. The Amputee Mobility Predictor: an instrument to assess determinants of the lower-limb amputee's ability to ambulate. *Arch. Phys. Med. Rehabil.* **83**, 613–627 (2002).
33. Riley, P. O., Paolini, G., Della Croce, U., Paylo, K. W. & Kerrigan, D. C. A kinematic and kinetic comparison of overground and treadmill walking in healthy subjects. *Gait Posture* **26**, 17–24 (2007).

Methods

Experimental protocol. Individuals with unilateral above-knee amputation were recruited from local clinics to participate in this study. Participant inclusion criteria included the following: age between 18 and 85 years, at least 6 months after amputation, daily use of their prescribed prosthesis and ability to walk on a treadmill without using the handrails. Exclusion criteria included serious comorbidities (including musculoskeletal, cardiac, neuromuscular, skin or vascular conditions) and inability to communicate and/or be understood by investigators. Following statistical power analysis, we enrolled six participants (4 male, 2 female; age, 33.8 ± 9.75 years; height, 1.74 ± 0.08 m; weight, 76.6 ± 16.1 kg; mean ± s.d.). All participants had prior experience with treadmill walking and were considered to be in class K3. Participant information is outlined in detail in Supplementary Table 1. The institutional review board at the University of Utah (IRB00099066) and the US Human Research Protection Office (HRPO) of the US Army Medical Research and Development Command (HSRRB log number: A-19840) approved the study protocol. Participants provided written informed consent to participate in the study. Participants also provided written consent for the use of pictures and videos of the experiments.

Upon arrival, participants donned a motion capture system based on inertial measurement units (lower body only; Awinda). After performing the motion capture system calibration[34], participants walked on a 12-m walkway ten times at their self-selected speed. Participants then donned a portable indirect calorimetry measurement system (K5, COSMED) and performed the final stage of the metabolic system calibration[35]. At the beginning of the experiment, participants stood still for 2 min while their baseline metabolic rate was collected. Next, the participants walked on a treadmill at 1 m s^{-1} for 6 min to assess the metabolic cost of walking without the exoskeleton (that is, "No Exo" condition). Participants were instructed not to touch the handrails. The experimenter made sure that they did not touch the handrails during the experiment. Using a fixed treadmill speed is common in studies aiming to assess metabolic rate[36]. The fixed speed of 1 m s^{-1} was selected because previous work[37] suggests that most individuals in class K3 can walk for 6 min at 1 m s^{-1} without using handrails or needing a break.

After the "No Exo" overground and "No Exo" treadmill tests were completed, the participants donned the powered hip exoskeleton. The motion capture system was recalibrated after the participant had donned the exoskeleton if the motion capture software indicated that this was necessary. The exoskeleton straps were adjusted as needed to alleviate any potential discomfort and to ensure proper fit for the participant. Then, the assistive controller was manually tuned by the experimenter for each participant to maximize assistance, in terms of energy injection, while ensuring the participant's comfort. Specifically, the experimenter adjusted the timing of flexion and extension peaks, as well as the peak torque in flexion and extension. To maximize assistance, the experimenter watched a real-time plot of the estimated joint power and changed the controller parameters while the participant walked with the exoskeleton. Comfort was assessed both by asking the participant for subjective feedback and by visually inspecting the participant's gait for abnormal patterns of socket movements. During tuning, the experimenter increased the assistance until the participant did not feel comfortable or movements of the socket or an abnormal gait pattern was noticed, and the assistance was then reduced to a comfortable level. Tuning and calibration took about 15 min, during which participants walked for less than 10 min in 2- to 3-min bouts.

After the exoskeleton was properly fit and tuned, participants rested for about 10 min, sitting or standing as preferred. Next, participants walked with the exoskeleton on the treadmill. As in the "No Exo" condition, participants were instructed not to touch the handrails. The experimenter made sure that they did not touch the handrails during the experiment. In previous studies, humans have taken about 20 min to adapt to walking with exoskeletons[38,39]. To allow sufficient time for learning, participants performed three treadmill walking sessions while wearing the exoskeleton. Each walking session consisted of a slow increase in assistance for 2 min, followed by 6 min of walking at the assistance level that had been previously selected for the participant. Thus, each participant experienced the exoskeleton assistance for 18 min. Data were collected during the last 2 min of the third walking session. Between each assisted session, the participants rested in a seated position until they felt ready to start a new walking session. Upon completion of the three exoskeleton walking sessions, the participants rested. After resting, we measured their standing metabolic expenditure to check for fatigue. After the treadmill test was completed, participants walked on a 12-m walkway at their preferred speed, with the same exoskeleton tuning that was used during the treadmill test. Each participant repeated the overground walking test ten times.

Randomizing the appearance of the exoskeleton and no exoskeleton conditions could have disrupted the adaptation period and introduced aftereffects[40]. This was also impractical because it would have required participants to repeatedly don and doff the exoskeleton, requiring additional time to ensure proper fit of the exoskeleton and recalibration of the motion capture system between sessions. Thus, the appearance of the conditions was not randomized, and the no-exoskeleton walking session was always performed first. However, the lack of randomization may have introduced bias. For example, if the participants became fatigued during the test, we would expect that their metabolic cost would have increased between the first and last 6-min walking sessions. To make sure fatigue was not a problem, we conducted a pilot experiment in which we recruited three individuals with above-knee amputation to perform four walking sessions at 1 m s^{-1}—the same walking speed used in the final experimental protocol—without the exoskeleton. The results of these experiments showed no significant difference in the metabolic cost of walking between sessions. The result of this pilot test suggests that the proposed experimental protocol did not cause fatigue in participants.

To assess potential drifts in respiratory measurements as well as fatigue over the duration of the experiment, we measured the standing metabolic expenditure before the no-exoskeleton tests and after the exoskeleton tests. We found no statistical difference between the standing metabolic expenditure measured at the beginning and at the end of the protocol. Thus, there were no significant drifts in respiratory measurement, and participants were not fatigued.

We asked one of the study participants (S3) to demonstrate donning and doffing the proposed autonomous powered hip exoskeleton without help, which is critical for usability in real life. As can be seen in Supplementary Video 3, the participant was able to don the exoskeleton in 25 s and doff the exoskeleton in 11 s.

Powered hip exoskeleton. The proposed powered hip exoskeleton is an evolution of the system preliminarily presented at a conference[18]. The exoskeleton uses offset slider-crank kinematics and is powered by a custom linear actuator comprising a brushless DC motor (EC-4pole 22, 24 V, 120 W, Maxon Motor) and a primary helical gear transmission (Boston Gear, 2.5:1 ratio) coupled with a high-efficiency ball screw (6-mm diameter, 2-mm lead, static-dynamic load rating of 1,700–2,300 N, efficiency >90%; Eichenberger). A linear guide (SSELBZ8, Misumi) supports the perpendicular load on the ball screw nut. Two angular contact ball bearings support radial and axial loads, respectively, on the helical gears. Translation of the screw nut and linear guide block along the rail is converted to rotation of the actuated hip joint through two 3D-printed composite compliant bars (Onyx with Fiberglass CFF, Markforged, stiffness 500 N mm^{-1}), creating a series elastic actuator. Lightweight, low-friction dry bushings (polytetrafluoroethylene bushing with steel shell, McMaster-Carr) support the load at the actuated hip joint. Sensing components include an inertial measurement unit (MPU 9250), a high-resolution incremental encoder (RM08, RLS) and a custom absolute encoder (AS5047U).

Custom pelvis and thigh orthoses were developed for the powered hip exoskeleton. Two flexible 3D-printed thermoplastic polyurethane (TPU) orthoses sit on the pelvis, with one on each side. The two orthoses are connected using BOA straps (Boa Technology), which have ratcheting dials to provide customizable tightening levels for the user. The pelvis orthoses are connected to the exoskeleton via a passive degree of freedom that allows for unconstrained hip abduction/adduction. Another 3D-printed TPU orthosis sits in the small of the back, held up by the BOA straps. A box containing the custom battery pack and controller unit is attached to the back pad using Velcro. The thigh orthosis is made of 2-inch webbing coated in a silicone adhesive to increase friction on the user's socket. Part of the thigh orthosis is made of latex rubber to provide elasticity because the webbing does not stretch. The thigh orthosis is secured to the socket by a strap with a buckle, and the strap length is adjusted as necessary. The thigh orthosis is connected to the carbon fiber frame of the exoskeleton through a prismatic passive degree of freedom (SSEBL6, Misumi). Combined, the passive degrees of freedom in the powered hip exoskeleton create a self-aligning mechanism, similar to the system described in our previous work[41], which has been shown to improve users' comfort[42]. The self-aligning mechanism minimizes the spurious forces and torques arising from any misalignment between the exoskeleton's powered flexion/extension axis and the user's anatomical flexion/extension axis. This self-aligning mechanism is particularly critical for users with amputations, because spurious forces and torques can result in loss of socket suspension, causing their prosthesis to shift and, potentially, fall off.

The custom control electronic units are contained in a 3D-printed case located on the user's lower back. A 32-bit microcontroller (Microchip Technology) performs the low-level sensor acquisition, the middle-level control algorithm, and low-level motor control at 1 kHz. Serial peripheral interface (SPI) buses are used to communicate with the IMU and a Raspberry Pi 3 module (Raspberry Pi Foundation), which runs the high-level controller, saves data, and communicates over Wi-Fi to a control computer that is used for exoskeleton assistance. Pulse-width modification (PWM) communicates the desired motor current to the motor driver (ESCON 50/5 Module, Maxon Motor), which performs the motor's lowest-level current control at 50 kHz. An eight-cell lithium-ion battery powers the custom control board and the motor. Voltage converters on the motherboard supply lower voltage to sensors and the microcontroller.

The stand-alone hip exoskeleton weighs 667 g, including three wiring cables connecting the electrical sensors and motors to the control board. The thigh orthosis, including the prismatic passive degree of freedom, weighs 116 g. The hip orthosis, including both 3D-printed pads, BOA straps, and the abduction and adduction passive degrees of freedom, weighs 925 g. The electronics box, including the controller and battery, weighs 743 g. The total weight of the exoskeleton, as used in the experiments, is 2,451 g.

Assistive controller. A hierarchical controller provides synchronous assistance during ambulation. At the high level, an adaptive frequency oscillator (AdOsc) estimates the

gait cadence of the coupled human–exoskeleton system, as well as the continuous phase evolution within the gait stride[43,44]. The AdOsc is a mathematical tool that enables the exoskeleton to synchronize with the human user's periodic movements. This mathematical tool was originally proposed for upper-limb exoskeletons[43] and has since been extensively validated with various lower-limb exoskeletons[12]. The AdOsc synchronizes with the user's movements to provide an accurate estimate of the gait cadence and delay-free estimates of the movement derivatives[45].

The cadence is combined with information about the start of the gait cycle to provide a continuous phase estimate, which is then used to synchronize the desired assistive torque with the user's gait. The start of the gait cycle is determined using the peak of the hip flexion angle. To detect peak flexion, we use a finite-state machine. The learned position signal from the AdOsc and the delay- and noise-free hip joint velocity estimates are used as the inputs to the finite-state machine. When the position signal crosses above a certain threshold (determined by the experimenter) and the velocity becomes negative, the peak of flexion is detected and the state transitions. In the next state, a peak of flexion is not allowed to be detected. To transition back into the state where peak flexion can once again be detected, the learned position signal must cross another threshold. At this point, a new peak can be obtained from the learned AdOsc signal. This finite-state machine approach enables the exoskeleton to reliably detect the peak flexion. The finite-state machine adds stability to the phase estimate from the AdOsc and, in turn, makes the assistance profiles more consistent. The adaptive oscillator automatically resets to 1 Hz before any movement by the participant.

Flexion and extension assistance profiles were generated using a summation of Gaussian functions. The Gaussian functions use the estimated gait phase to apply Gaussian-shaped assistance based on the percent of gait cycle. The experimenter can manually adjust the characteristics of the assistance online. Timing of the peak assistance, assistance width and peak assistance amplitude are selected for both flexion and extension assistance. The low-level controller, finally, converts the desired hip assistance values into desired motor torque and sends the appropriate commands to the motor driver.

Reporting Summary. Further information on research design is available in the Nature Research Reporting Summary linked to this article.

Data availability

All data are freely available in an open repository[19].

Code availability

Code is freely available upon written request to the corresponding author.

References

34. Zhang, J.-T., Novak, A. C., Brouwer, B. & Li, Q. Concurrent validation of Xsens MVN measurement of lower limb joint angular kinematics. *Physiol. Meas.* **34**, N63–N69 (2013).
35. Guidetti, L. et al. Validity, reliability and minimum detectable change of COSMED K5 portable gas exchange system in breath-by-breath mode. *PLoS ONE* **13**, e0209925 (2018).
36. Sawicki, G. S., Beck, O. N., Kang, I. & Young, A. J. The exoskeleton expansion: improving walking and running economy. *J. Neuroeng. Rehabil.* **17**, 25 (2020).
37. Hood, S., Ishmael, M. K., Gunnell, A., Foreman, K. B. & Lenzi, T. A kinematic and kinetic dataset of 18 above-knee amputees walking at various speeds. *Sci. Data* **7**, 150 (2020).
38. Collins, S. H., Wiggin, M. B. & Sawicki, G. S. Reducing the energy cost of human walking using an unpowered exoskeleton. *Nature* **522**, 212–215 (2015).
39. Galle, S., Malcolm, P., Derave, W. & De Clercq, D. Adaptation to walking with an exoskeleton that assists ankle extension. *Gait Posture* **38**, 495–499 (2013).
40. Reinkensmeyer, D., Wynne, J. H. & Harkema, S. J. A robotic tool for studying locomotor adaptation and rehabilitation. in *Proceedings of the Second Joint 24th Annual Conference and the Annual Fall Meeting of the Biomedical Engineering Society* **3**, 2353–2354 (Engineering in Medicine and Biology, 2002); https://doi.org/10.1109/IEMBS.2002.1053318
41. Sarkisian, S. V., Ishmael, M. K., Hunt, G. R. & Lenzi, T. Design, development, and validation of a self-aligning mechanism for high-torque powered knee exoskeletons. *IEEE Trans. Med. Robot. Bionics* **2**, 248–259 (2020).
42. Sarkisian, S. V., Ishmael, M. K. & Lenzi, T. Self-aligning mechanism improves comfort and performance with a powered knee exoskeleton. *IEEE Trans. Neural Syst. Rehabil. Eng.* **29**, 629–640 (2021).
43. Ronsse, R. et al. Human–robot synchrony: flexible assistance using adaptive oscillators. *IEEE Trans. Biomed. Eng.* **58**, 1001–1012 (2011).
44. Lenzi, T., Carrozza, M. C. & Agrawal, S. K. Powered hip exoskeletons can reduce the user's hip and ankle muscle activations during walking. *IEEE Trans. Neural Syst. Rehabil. Eng.* **21**, 938–948 (2013).
45. Ronsse, R. et al. Real-time estimate of velocity and acceleration of quasi-periodic signals using adaptive oscillators. *IEEE Trans. Robot.* **29**, 783–791 (2013).

Acknowledgements

We wish to acknowledge the contribution of all study participants. We would like to thank M. Tran, S. Sarkisian and C. Buchanan for their help with the development of the powered hip exoskeleton and related interfaces. We would like to thank J. Mendez for assistance in collection and processing of all data from participants and G. Hunt for help proofreading the manuscript. We would also like to thank C. Hansen and C. Duncan for their help with participant recruitment. Funding for this study was provided by the Congressionally Directed Medical Research Program of the Department of Defense under grant number W81XWH-16-1-0701 awarded to T.L. and by the National Science Foundation under grant number 2046287 awarded to T.L.

Author contributions

T.L. directed the project. T.L. and M.K.I. invented the controller and implemented it on the powered hip exoskeleton. M.K.I., D.A. and T.L. conducted the experiments with human participants. M.K.I. and D.A. analyzed the data. All authors contributed to manuscript preparation.

Competing interests

The authors declare no competing interests.

Additional information

Supplementary information The online version contains supplementary material available at https://doi.org/10.1038/s41591-021-01515-2.

Correspondence and requests for materials should be addressed to Tommaso Lenzi.

Peer review information *Nature Medicine* thanks Gregory Sawicki and the other, anonymous, reviewer(s) for their contribution to the peer review of this work. Michael Basson was the primary editor on this article and managed its editorial process and peer review in collaboration with the rest of the editorial team.

Reprints and permissions information is available at www.nature.com/reprints.

nature research

Corresponding author(s): Tommaso Lenzi

Last updated by author(s): Aug 13, 2021

Reporting Summary

Nature Research wishes to improve the reproducibility of the work that we publish. This form provides structure for consistency and transparency in reporting. For further information on Nature Research policies, see our Editorial Policies and the Editorial Policy Checklist.

Statistics

For all statistical analyses, confirm that the following items are present in the figure legend, table legend, main text, or Methods section.

n/a	Confirmed	
☐	☒	The exact sample size (*n*) for each experimental group/condition, given as a discrete number and unit of measurement
☐	☒	A statement on whether measurements were taken from distinct samples or whether the same sample was measured repeatedly
☐	☒	The statistical test(s) used AND whether they are one- or two-sided *Only common tests should be described solely by name; describe more complex techniques in the Methods section.*
☐	☒	A description of all covariates tested
☐	☒	A description of any assumptions or corrections, such as tests of normality and adjustment for multiple comparisons
☐	☒	A full description of the statistical parameters including central tendency (e.g. means) or other basic estimates (e.g. regression coefficient) AND variation (e.g. standard deviation) or associated estimates of uncertainty (e.g. confidence intervals)
☐	☒	For null hypothesis testing, the test statistic (e.g. *F*, *t*, *r*) with confidence intervals, effect sizes, degrees of freedom and *P* value noted *Give P values as exact values whenever suitable.*
☒	☐	For Bayesian analysis, information on the choice of priors and Markov chain Monte Carlo settings
☒	☐	For hierarchical and complex designs, identification of the appropriate level for tests and full reporting of outcomes
☒	☐	Estimates of effect sizes (e.g. Cohen's *d*, Pearson's *r*), indicating how they were calculated

Our web collection on statistics for biologists contains articles on many of the points above.

Software and code

Policy information about availability of computer code

Data collection	COSMED Omnia 1.6.7 was used to collect data from the K5 metabolic system. LabVIEW 2020 was used to simultaneously control and collect data from the hip exoskeleton. Xsens MNV Studio 2020.0.0 was used to collect kinematics data.
Data analysis	The data were analyzed offline using MATLAB R2021a.

For manuscripts utilizing custom algorithms or software that are central to the research but not yet described in published literature, software must be made available to editors and reviewers. We strongly encourage code deposition in a community repository (e.g. GitHub). See the Nature Research guidelines for submitting code & software for further information.

Data

Policy information about availability of data

All manuscripts must include a data availability statement. This statement should provide the following information, where applicable:

- Accession codes, unique identifiers, or web links for publicly available datasets
- A list of figures that have associated raw data
- A description of any restrictions on data availability

All figures, excluding Figure 1, have associated data. The data for these figures is calculated from a subset of the data provided, as described in the manuscript. Subject identifiers are used to retain anonymity. All data is made open on Figshare: https://doi.org/10.6084/m9.figshare.15180711 .

Field-specific reporting

Please select the one below that is the best fit for your research. If you are not sure, read the appropriate sections before making your selection.

☒ Life sciences ☐ Behavioural & social sciences ☐ Ecological, evolutionary & environmental sciences

For a reference copy of the document with all sections, see nature.com/documents/nr-reporting-summary-flat.pdf

Life sciences study design

All studies must disclose on these points even when the disclosure is negative.

Sample size	The statistical analysis shows that the proposed longitudinal study design with only two groups (i.e., with and without the exoskeleton) allows for a statistical power of 90% with a sample size of six participants and a minimum detectable effect of 9.6%.
Data exclusions	Metabolic data was excluded if the trial needed to be stopped due to sensor slipping, subject discomfort, etc. Exoskeleton data was excluded if the collection began or concluded within the stride.
Replication	We provided a detailed description of the instruments used for metabolic and kinematic data collection, which are available on the market. We provided a detailed description of the design of the custom powered hip exoskeleton and the assistive torque profile used for each study participant. The experimental tuning procedure is described in the methods section. Replication of the result was successful when participants where allowed to lightly touch the treadmill handrails, which was not the case for the present protocol.
Randomization	We use a longitudinal study design in which all participants performed the treadmill and overground tests with and without the powered hip exoskeleton. All participant performed the walking test without the exoskeleton first in order not to break the adaptation period to the exoskeleton and to avoid the recalibration of the kinematic system.
Blinding	Blinding was not possible due to the nature of wearing a powered exoskeleton.

Reporting for specific materials, systems and methods

We require information from authors about some types of materials, experimental systems and methods used in many studies. Here, indicate whether each material, system or method listed is relevant to your study. If you are not sure if a list item applies to your research, read the appropriate section before selecting a response.

Materials & experimental systems

n/a	Involved in the study
☒	☐ Antibodies
☒	☐ Eukaryotic cell lines
☒	☐ Palaeontology and archaeology
☒	☐ Animals and other organisms
☐	☒ Human research participants
☒	☐ Clinical data
☒	☐ Dual use research of concern

Methods

n/a	Involved in the study
☒	☐ ChIP-seq
☒	☐ Flow cytometry
☒	☐ MRI-based neuroimaging

Human research participants

Policy information about studies involving human research participants

Population characteristics	Relevant covariate characteristics of the participant population have been included in the study.
Recruitment	Participants for this study were selected based on a set of inclusion/exclusion criteria. We required subjects to be transfemoral amputees at a K3 ambulation classification, at least 1 year post operation, between the ages of 18 and 80, have been using their prescribed prosthesis for 6 months, use their prescribed prosthesis for at least 3 hours a day, and can walk with or without the use of an assistive device. Participants were excluded from the study if they were over 250 lbs, inactive, had a cognitive deficiency that precluded the ability to provide informed consent, pregnancy, or a co-morbidity that interfered with the study. Selection bias were abated through the use of these selection criteria.
Ethics oversight	The Institutional Review Board at the University of Utah (IRB00099066) and the US Human Research Protection Office (HRPO) of the US Army Medical Research and Development Command (HSRRB Log Number: A-19840) have approved the study protocol.

Note that full information on the approval of the study protocol must also be provided in the manuscript.